Human Molecular Genetics, 2004, Vol. 13, No. 1 **69–78**
DOI: 10.1093/hmg/ddh011
Advance Access published on November 12, 2003

Proline to arginine mutations in FGF receptors 1 and 3 result in Pfeiffer and Muenke craniosynostosis syndromes through enhancement of FGF binding affinity

Omar A. Ibrahimi[1], Fuming Zhang[2], Anna V. Eliseenkova[1], Robert J. Linhardt[2] and Moosa Mohammadi[1,*]

[1]Department of Pharmacology, New York University School of Medicine, New York, NY 10016, USA and
[2]Department of Chemistry, Biology, and Chemical and Biological Engineering, Rensselaer Polytechnic Institute, Troy, NY 12180, USA

Received August 18, 2003; Revised October 22, 2003; Accepted November 3, 2003

Identical proline→arginine gain-of-function mutations in fibroblast growth factor receptor (FGFR) 1 (Pro252Arg), FGFR2 (Pro253Arg) and FGFR3 (Pro250Arg), result in type I Pfeiffer, Apert and Muenke craniosynostosis syndromes, respectively. Here, we characterize the effects of proline→arginine mutations in FGFR1c and FGFR3c on ligand binding using surface plasmon resonance and X-ray crystallography. Both Pro252Arg FGFR1c and Pro250Arg FGFR3c exhibit an enhancement in ligand binding in comparison to their respective wild-type receptors. Interestingly, binding of both mutant receptors to FGF9 was notably enhanced and implicates FGF9 as a potential pathophysiological ligand for mutant FGFRs in mediating craniosynostosis. The crystal structure, of Pro252Arg FGFR1c in complex with FGF2, demonstrates that the enhanced ligand binding is due to an additional set of receptor-ligand hydrogen bonds, similar to those gain-of-function interactions that occur in the Apert syndrome Pro253Arg FGFR2c-FGF2 crystal structure. However, unlike the Apert syndrome Pro253Arg FGFR2c mutant, neither the Pfeiffer syndrome Pro250Arg FGFR1c mutant nor the Muenke syndrome Pro250Arg FGFR3c mutant bound appreciably to FGF7 or FGF10. This observation provides a potential explanation for why the limb phenotypes, observed in type I Pfeiffer and Muenke syndromes, are less severe than the limb abnormalities observed in Apert syndrome. Hence, although analogous proline→arginine mutations in FGFR1-3 act through a common structural mechanism to result in gain-of-function, differences in the primary sequence among FGFRs result in varying effects on ligand binding specificity.

INTRODUCTION

The fibroblast growth factor (FGF) receptor (FGFR) family consists of four single-pass transmembrane receptor tyrosine kinases, FGFR1-4 (1,2). The extracellular portion of FGFRs mediates ligand binding and consists of three immunoglobulin (Ig)-like domains (D1–D3). Tissue specific alternative splicing of the second half of D3 in FGFR1-3 creates 'b' and 'c' isoforms and plays a major role in determining the binding profile of each receptor to the 18 known FGF ligands (excluding FHFs) (1–3). Heparin or heparan sulfate proteoglycan is an obligatory cofactor for receptor binding and dimerization, the initial steps in FGFR activation (4–7).

Craniosynostosis, the premature fusion of one or more cranial sutures, is a common clinical finding that occurs in ~1/2500 births (8). Mutations in FGFR1-3 are responsible for several craniosynostosis syndromes including Apert syndrome (AS), Beare-Stevenson syndrome, Crouzon syndrome, Jackson–Weiss syndrome, Muenke syndrome (MS) and Pfeiffer syndrome (PS) (9,10). The etiology of FGFR related skeletal disorders stems from receptor gain-of-function, either through a ligand-independent or ligand-dependent manner. Ligand-independent gain-of-function may arise from mutations resulting in: (i) covalent receptor dimerization (11–13); (ii) non-covalent receptor dimerization (14,15); or (iii) stabilization of the active conformation of the kinase domain (15,16). In

*To whom correspondence should be addressed. Tel: +1 2122632907; Fax: +1 2122637133; Email: mohammad@saturn.med.nyu.edu

contrast, ligand-dependent gain-of-function may result from mutations causing: (i) enhanced ligand binding affinity (17,18); (ii) loss of ligand binding specificity (19); or (iii) ectopic expression of inappropriate splice isoforms (20).

Mutations of a highly conserved Ser-Pro dipeptide motif in the D2–D3 linker region account for the most common of the craniosynostosis syndromes. Interestingly, these mutations have the highest rates for transversions known in the human genome (8). AS results almost exclusively from one or the other of two missense mutations, Ser252Trp or Pro253Arg, in FGFR2 (21). It is the most severe of the craniosynostosis syndromes and is additionally characterized by syndactyly of the hands and feet. Type I PS and MS result from Pro252Arg and Pro250Arg mutations in FGFR1 and FGFR3, respectively (22,23). In contrast to AS, type I PS and MS are characterized by mild limb phenotypes (8,24).

The AS mutations, Ser252Trp and Pro253Arg in FGFR2, are the most well-characterized of the D2–D3 linker region craniosynostosis mutations. Because these mutations occur prior to the alternatively spliced D3 region, both the 'b' and 'c' splice isoforms are affected. However, most studies have focused on the 'c' splice isoform since histological analysis of AS tissues suggests that the majority of pathology occurs in mesenchymal tissue that expresses the 'c' splice isoform of FGFRs (25). Initial evidence suggesting how these mutations may result in receptor gain-of-function came from ligand binding studies of wild type and AS mutant FGFR2c in which the mutant receptors displayed enhanced binding to FGF2 (17). A later report demonstrated that each AS mutant FGFR2c does not bind FGF2 better than wild-type FGFR2c (19). Instead, it was shown that AS mutations result in the loss of FGFR2 ligand specificity (19). Normally, mesenchymally expressed FGFR2c binds to FGF2 but does not bind to FGF7 or FGF10. Conversely, epithelial FGFR2b binds to FGF7 and FGF10 but has weak affinity for FGF2 (26–28). This specificity permits directional epithelial-mesenchymal signaling to occur during organogenesis and limb development. However, AS Ser252Trp and Pro253Arg mutations in FGFR2c enabled FGF7 binding, thus suggesting that some of the severe and unique phenotypes in AS may result from pathophysiological disruption of normal signaling networks by inappropriate autocrine activation (19).

We recently reported the crystal structures of each AS mutant FGFR2c in complex with FGF2 (18). Both Ser252Trp FGFR2c and Pro253Arg FGFR2c engage FGF2 with distinct additional contacts, thereby providing a structural basis for receptor gain-of-function. These structures and sequence alignment of the FGF family suggests that the Pro253Arg mutation, and to a lesser extent the Ser252Trp mutation, result in generalized enhancement of ligand binding and hence may even enable the binding of FGFs that are outside of the normal receptor binding spectrum.

To date, the molecular mechanism by which the corresponding proline→arginine mutations in FGFR1 and FGFR3 result in PS and MS, respectively, have not been characterized, although a mouse model for PS has provided direct genetic evidence that the Pro252Arg mutation in FGFR1 is causative for PS (29). In this report, we examine the mechanisms by which Pro252Arg and Pro250Arg mutations activate FGFR1c and FGFR3c, respectively, using surface plasmon resonance (SPR) and X-ray crystallography. Here, we show that these mutations result in the enhancement of FGF binding affinity, but are not sufficient to override FGFR1c and FGFR3c ligand binding specificity.

RESULTS AND DISCUSSION

Several FGFR ligand binding studies have been reported that employ a variety of techniques including radiolabeled ligand competition binding, SPR, and isothermal titration calorimetry assays (17,30–33). However, these studies are limited in that they focus on only a few interactions, and since they utilize different techniques, comparisons between studies are difficult. Hence, in order to quantify mutant FGFR–FGF interactions, we measured the binding of wild-type and Pro252Arg FGFR1c and wild-type and Pro250Arg FGFR3c to FGF1-10 using SPR. FGF8 was found to aggregate on the biosensor surface and therefore FGFR–FGF8 interactions could not be analyzed using SPR. The kinetic data are summarized in Table 1 and, to our knowledge, are the most comprehensive ligand binding studies reported for FGFR1c and FGFR3c.

Wild-type FGFR1c bound with high affinity to FGF1, FGF2, FGF4 and FGF6 but with poor affinity to FGF9 (Fig. 1A, C, E and I, Table 1). These findings are in agreement with prior binding and mitogenic response assays for FGFR1c (3,17,30–34). In contrast, wild-type FGFR1c did not bind to FGF3, FGF7 and FGF10, ligands which preferentially signal through FGFR2b (Fig. 1G; Table 1) (3). We did not detect binding of FGF5 to wild-type FGFR1c (Table 1). Wild-type FGFR1c–FGF5 binding has not been previously demonstrated although FGF5 is moderately mitogenic for FGFR1c BaF3 cells (3). Interestingly, compared to wild-type FGFR1c, the PS Pro252Arg FGFR1c mutant displayed a generalized 2- to 5-fold increase in binding affinity for FGF1, FGF2, FGF4, and FGF6 (Fig. 1A, B, C, D, E and F, Table 1). A notable exception was FGF9, which had a striking 30-fold increase in binding affinity for the mutant FGFR1c (Fig. 1I and J Table 1). The enhanced binding in almost all cases could be attributed to both faster association rates (K_{on}) and slower dissociation kinetics (K_{off}) (Table 1).

In the case of wild-type FGFR3c, high affinity binding was observed only to FGF1 (Fig. 2A; Table 1), but not to other FGFs examined. The lack of binding of FGF3, FGF7 and FGF10 to wild-type FGFR3c is consistent with the preferential signaling of these FGFs through FGFR2b (3). Other studies have also detected poor FGFR3c binding to FGF2 (35–37), FGF4 and FGF6 (37). Additionally, studies of BaF3 cells expressing FGFR3 show negligible to modest mitogenic responses to FGF2, FGF4, FGF6 and FGF9 (38), although FGF2, FGF4 and FGF9 strongly activate BaF3 cells expressing a chimeric FGFR3c-FGFR1c construct (3). It is possible that the chimeric FGFR3c–FGFR1c construct used by Ornitz *et al.* (3) masks differences in FGFR3c ligand binding due to signal overamplification by the inherently more active FGFR1c kinase domain.

The MS Pro250Arg FGFR3c mutant also displayed an increase in ligand binding affinity (Fig. 2; Table 1). FGF1 displays a nearly 2-fold increase in binding affinity for Pro250Arg FGFR3c over wild-type FGFR3c (Fig. 2A and B, Table 1). Additionally, the Pro250Arg mutation permits

Table 1. Summary of kinetic data

FGF		FGFR1c		FGFR3c	
		Wild-type	Pro252Arg	Wild-type	Pro250Arg
FGF1	K_{on} (/M/s)[a]	2.24×10^5	5.6×10^5	8.79×10^5	8.92×10^5
	K_{off} (/s)[a]	3.05×10^{-2}	1.71×10^{-2}	2.02×10^{-1}	1.15×10^{-1}
	K_D (M)[b]	1.36×10^{-7}	3.05×10^{-8}	2.30×10^{-7}	1.28×10^{-7}
FGF2	K_{on} (/M/s)	9.64×10^4	1.77×10^5	NB	4.01×10^5
	K_{off} (/s)	5.96×10^{-3}	4.30×10^{-3}	NB	4.10×10^{-1}
	K_D (M)	6.19×10^{-8}	2.44×10^{-8}	NB	1.02×10^{-6}
FGF3	K_{on} (/M/s)	NB[c]	NB	NB	NB
	K_{off} (/s)	NB	NB	NB	NB
	K_D (M)	NB	NB	NB	NB
FGF4	K_{on} (/M/s)	2.62×10^5	5.97×10^5	NB	NB
	K_{off} (/s)	4.33×10^{-2}	4.41×10^{-2}	NB	NB
	K_D (M)	1.65×10^{-7}	7.39×10^{-8}	NB	NB
FGF5	K_{on} (/M/s)	NB	NB	NB	NB
	K_{off} (/s)	NB	NB	NB	NB
	K_D (M)	NB	NB	NB	NB
FGF6	K_{on} (/M/s)	2.93×10^5	5.07×10^5	NB	NB
	K_{off} (/s)	3.05×10^{-2}	1.88×10^{-2}	NB	NB
	K_D (M)	1.04×10^{-7}	3.71×10^{-8}	NB	NB
FGF7	K_{on} (/M/s)	NB	NB	NB	NB
	K_{off} (/s)	NB	NB	NB	NB
	K_D (M)	NB	NB	NB	NB
FGF9	K_{on} (/M/s)	3.44×10^4	5.58×10^5	NB	5.63×10^4
	K_{off} (/s)	4.15×10^{-2}	2.26×10^{-2}	NB	4.58×10^{-3}
	K_D (M)	1.21×10^{-6}	4.05×10^{-8}	NB	8.14×10^{-8}
FGF10	K_{on} (/M/s)	NB	NB	NB	NB
	K_{off} (/s)	NB	NB	NB	NB
	K_D (M)	NB	NB	NB	NB

[a]K_{on} and K_{off} were derived as described in Materials and Methods. χ^2 was less than 10% of R_{max} in all cases.
[b]The apparent affinity, K_D, is equal to K_{off}/K_{on}.
[c]NB, negligible binding.

FGFR3c to weakly bind FGF2, whereas wild-type FGFR3c binds FGF2 negligibly (Fig. 2C and D; Table 1). Interestingly, as in the case of FGFR1c, the proline→arginine mutation enables FGFR3c to bind FGF9 with high affinity while FGF9 binding to wild-type FGFR3c is negligible (Fig. 2I and J; Table 1). This robust increase in FGF9 binding has also been qualitatively observed by size exclusion chromatography (data not shown).

To ascertain the structural basis for the enhanced affinity of Pro252Arg FGFR1c and Pro250Arg FGFR3c mutants towards FGFs, we chose to crystallize each mutant receptor with FGF ligand. We were able to successfully generate diffracting crystals of Pro252Arg FGFR1c–FGF2. The crystal structure of Pro252Arg FGFR1c–FGF2 was solved using molecular replacement. Data collection and refinement statistics are given in Tables 2 and 3. The overall structure of the Pro252Arg FGFR1c–FGF2 complex is identical to the structure of the wild-type FGFR1c–FGF2 complex. The relative orientation between D2 and D3 is unaffected by the proline→arginine mutation. Two 1:1 FGFR1c–FGF2 complexes compose the asymmetric unit and form a symmetric dimer.

In both copies of Pro252Arg FGFR1c–FGF2, the guanidinium group of Arg-252 in FGFR1c makes three hydrogen bonds with the β8–β9 turn of FGF2 (Fig. 3). Two hydrogen bonds are made with the backbone carbonyl oxygens of Leu-107 and Glu-108 of FGF2 and a third with the side chain amide group of Asn-111 of FGF2. Thus, the structural basis for the enhanced binding of Pro252Arg FGFR1c to FGF2 is the presence of additional receptor–ligand interactions that are not present in the wild-type FGFR1c–FGF2 structure. Interestingly, these gain-of-function contacts are similar to the additional contacts made between the AS Pro253Arg FGFR2c mutant and FGF2 (18). Since two of the three additional hydrogen bonds involve backbone carbonyl oxygens of FGF2, these interactions should also occur with other FGFs and explains the generalized enhancement of FGF binding affinity by proline→arginine mutant FGFRs (Table 1). We predict that these proline→arginine mutant FGFRs should also display enhanced binding to FGF16-23, which have not yet been analyzed for binding.

Interestingly, the exceptional increase in binding affinity of FGF9 for Pro252Arg FGFR1c and Pro253Arg FGFR3c implicates FGF9 as a potential pathophysiological ligand for craniosynostosis mediated by D2–D3 linker region mutants. Indeed, FGF9 is expressed at extremely high levels in the cranial suture and has been shown to stimulate the mesenchymally expressed 'c' isoform of FGFR1-3 (3,39,40).

Table 2. Summary of crystallographic analysis: data collection statistics

Resolution (Å)	Reflections (total/unique)	Completeness (%)	R_{sym}[a] (%)	Signal ($\langle I/\sigma I \rangle$)
30.0–2.9	134842/22295	99.7 (99.9)[b]	11.7 (37.4)[b]	13.1

[a]$R_{sym} = 100 \times \Sigma_{hkl}\Sigma_i|I_i(hkl) - \langle I(hkl)\rangle|/\Sigma_{hkl}\Sigma_i I_i(hkl)$.
[b]Value in parentheses is for the highest resolution shell: 3.0–2.9 Å.

Table 3. Summary of crystallographic analysis: refinement statistics[a]

Resolution (Å)	Reflections	R_{cryst}/R_{free}[b](%)	Root-mean-square deviations		B-factors[c] (Å^2)
			Bonds (Å)	Angles (°)	
25.0–2.9	21918	26.7–31.8	0.009	1.5	0.64

[a]Atomic model: 5161 protein atoms and 4 SO_4 ions.
[b]$R_{cyst/free} = 100 \times \Sigma_{hkl} \| F_o(hkl)| - |F_c(hkl) \| / \Sigma_{hkl}|F_o(hkl)|$, where F_o ($>0\sigma$) and F_c are the observed and calculated structure factors, respectively, 10% of the reflections were used for calculation of R_{free}.
[c]For bonded protein atoms.

However, since our SPR analysis did not include every FGF, the possibility of another FGF that exhibits a robust enhancement in binding mutant FGFRs cannot be ruled out. Nonetheless, in order for any FGF to be pathophysiologically relevant in mediating craniosynostosis, it must also be expressed in the cranial sutures and capable of activating FGFR1-3.

The crystal structure of FGF9 provides an explanation as to why the increase in binding affinity of FGF9 for mutant receptors is so marked in comparison to other FGFs examined (41). FGF9 activity is proposed to be regulated through an autoinhibitory mechanism that stems from its ability to dimerize. Dimerization of FGF9 involves the N- and C-terminal regions of FGF9, as well as the β-trefoil core region, thereby occluding a major portion of the receptor binding interface. Notably, the β8–β9 turn of FGF9, part of the core region involved in FGF9 dimerization, is also the region of FGF ligand that is predicted to engage in additional contacts with proline→arginine mutant FGFRs. It is likely that the balance between FGF9 auto-inhibition and receptor binding is shifted to favor the latter due to enhanced interaction of mutant FGFRs with the β8–β9 turn of FGF9. Such an effect is consistent with the binding kinetics of FGF9 to wild-type and mutant FGFR1c (Table 1). The large increase in association rate (K_{on}) of the Pro252Arg FGFR1c–FGF9 interaction, relative to the wild-type FGFR1c–FGF9 interaction, is not observed for other FGFs and is harmonious with the above hypothesis. Similarly, the reduction in dissociation rate (K_{off}) for the Pro252Arg FGFR1c–FGF9 interaction, relative to the wild-type FGFR1c–FGF9 interaction, is similar for other FGFs and suggests that mutant receptor–FGF9 complexes are stabilized through similar additional contacts. However, validation of this hypothesis requires additional experimental analysis.

FGF9 knockout mice have been recently reported (42), but since suture closure normally occurs between P25 and P45 in mice (43) and FGF9 knockout mice die at birth, little can be inferred about the role of FGF9 in cranial suture signaling. However, these mice are notable in that they display male-to-female sex reversal, thereby implicating FGF9 as a central player in testicular development (42). Paradoxically, while FGFR mutations are deleterious for skeletal development, several recent studies provide evidence that certain mutations in FGFR2-3 confer a selective advantage to male sperm cells (44–46). FGFs, perhaps FGF9, may mediate this selective advantage in the case of ligand-dependent FGFR mutations by enhancing FGF–FGFR binding.

Interestingly, craniosynostosis syndromes resulting from proline→arginine mutations in FGFR1 and FGFR3, type I PS and MS, respectively, are characterized by very mild limb pathology in contrast to AS (8,24). Both AS mutations have been shown to enable FGFR2c to bind FGF7 (19), with the Pro253Arg substitution demonstrating a stronger effect and correlating with the more severe syndactyly observed in Pro253Arg AS patients (47–49). Hence, it is currently thought that limb abnormalities in AS arise from autocrine activation of FGFR2c by FGF7 or a similar FGF, although mutant FGFR2c–FGF7 binding has not yet been examined using SPR. Based on the data of Ornitz *et al.* (3), our inability to detect binding of corresponding proline→arginine mutations in FGFR1c and FGFR3c to bind FGF7 or FGF10 (Table 1; Figs 1H and 2H) seems to be consistent with the absence of severe limb phenotypes in type I PS and MS.

The recent crystal structure of FGFR2b–FGF10 provides a structural basis for why these mutations in FGFR1c and FGFR3c do not result in FGF7 binding. In this structure, several D2 residues that are conserved only in FGFR2 are critical for D2-FGF10 binding (50). The lack of conservation of these residue in FGFR1 and FGFR3 suggests that even if corresponding proline→arginine mutations were to introduce additional receptor-ligand contacts they may not be sufficient to enable either mutant FGFR1c or FGFR3c to bind to FGF7. Alternatively, the differences in limb phenotype between these three craniosynostosis syndromes may be due to the distinct roles of FGFR1-3 in limb development. Nevertheless, additional factors must play a role, since some FGFR2 mutations result in craniosynostosis with mild limb phenotypes.

CONCLUDING REMARKS

The results presented here indicate that analogous proline→arginine mutations in the D2–D3 linker region of FGFR1c and FGFR3c result in PS and MS, respectively, through an enhancement of FGF binding. The structural basis for this enhanced binding is the additional interactions that occur between the β8–β9 turn of FGF ligand and the mutated proline→arginine residue of FGFR. The striking enhancement of FGF9 binding in the case of Pro252Arg FGFR1c and Pro250Arg FGFR3c, in comparison to respective wild type FGFRs, points to FGF9 as a potential pathophysiological ligand in mediating craniosynostosis. Importantly, the lack of binding of Pro252Arg FGFR1c and Pro250Arg FGFR3c to FGF7 or FGF10 provides an explanation for the mild limb phenotypes in type I PS and MS. Moreover, the specific involvement of these mutations with the β8–β9 turn of FGF allows for the design of antagonist and agonist of FGF signaling that may hold therapeutic value for the treatment

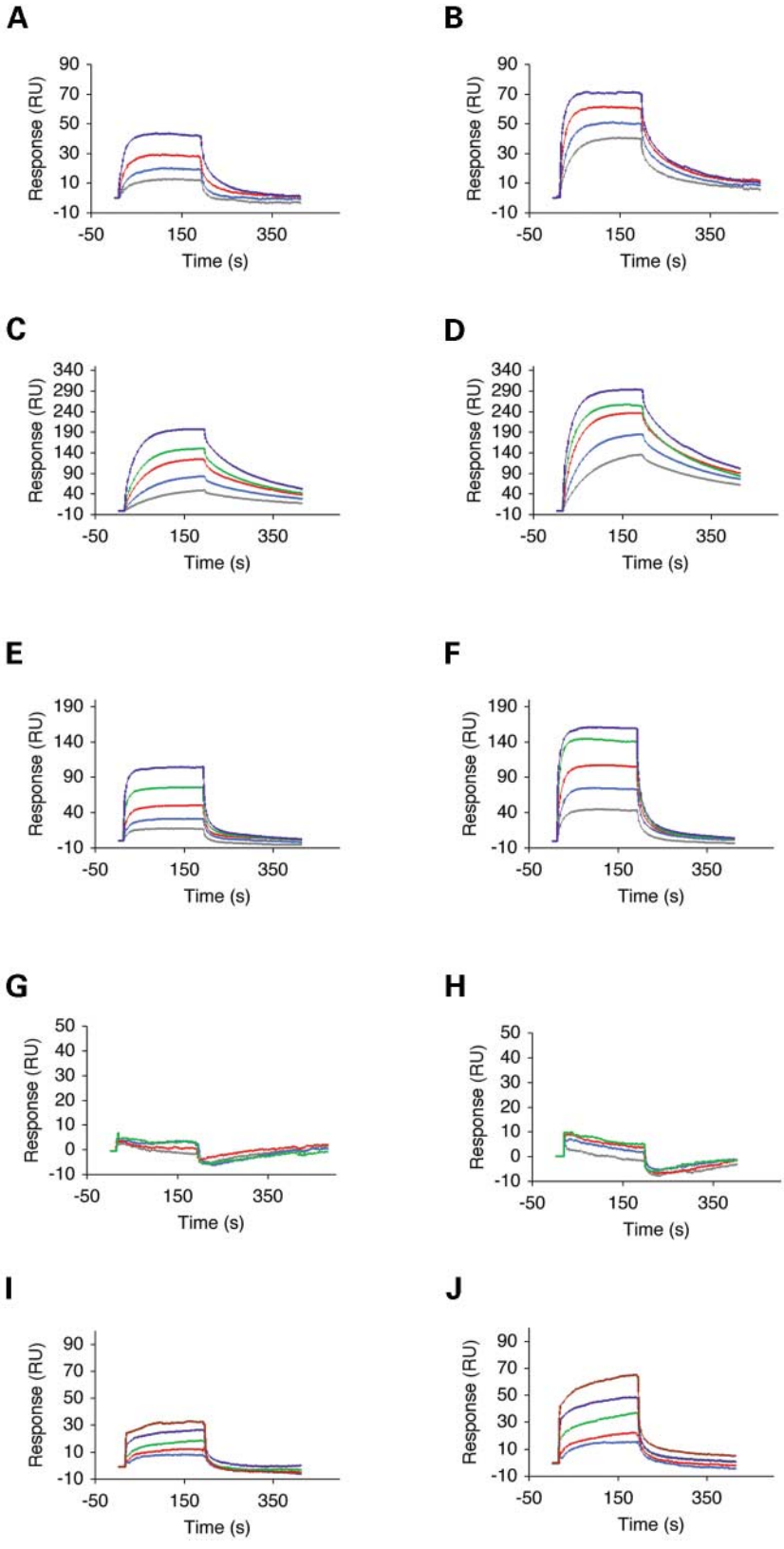

Figure 1. Surface plasmon resonance analysis of FGFR1c–FGF interactions. Sensorgrams of wild-type and Pro252Arg FGFR1c, respectively, binding to FGF1 (**A** and **B**), FGF2 (**C** and **D**), FGF4 (**E** and **F**), FGF7 (**G** and **H**) and FGF9 (**I** and **J**). Analyte concentrations are colored as follows: 25 nM in gray, 50 nM in blue, 100 nM in red, 200 nM in green, 400 nM in violet and 800 nM in brown. The biosensor chip response is indicated on the *y*-axis (ΔRU) as a function of time (*x*-axis) at 25°C.

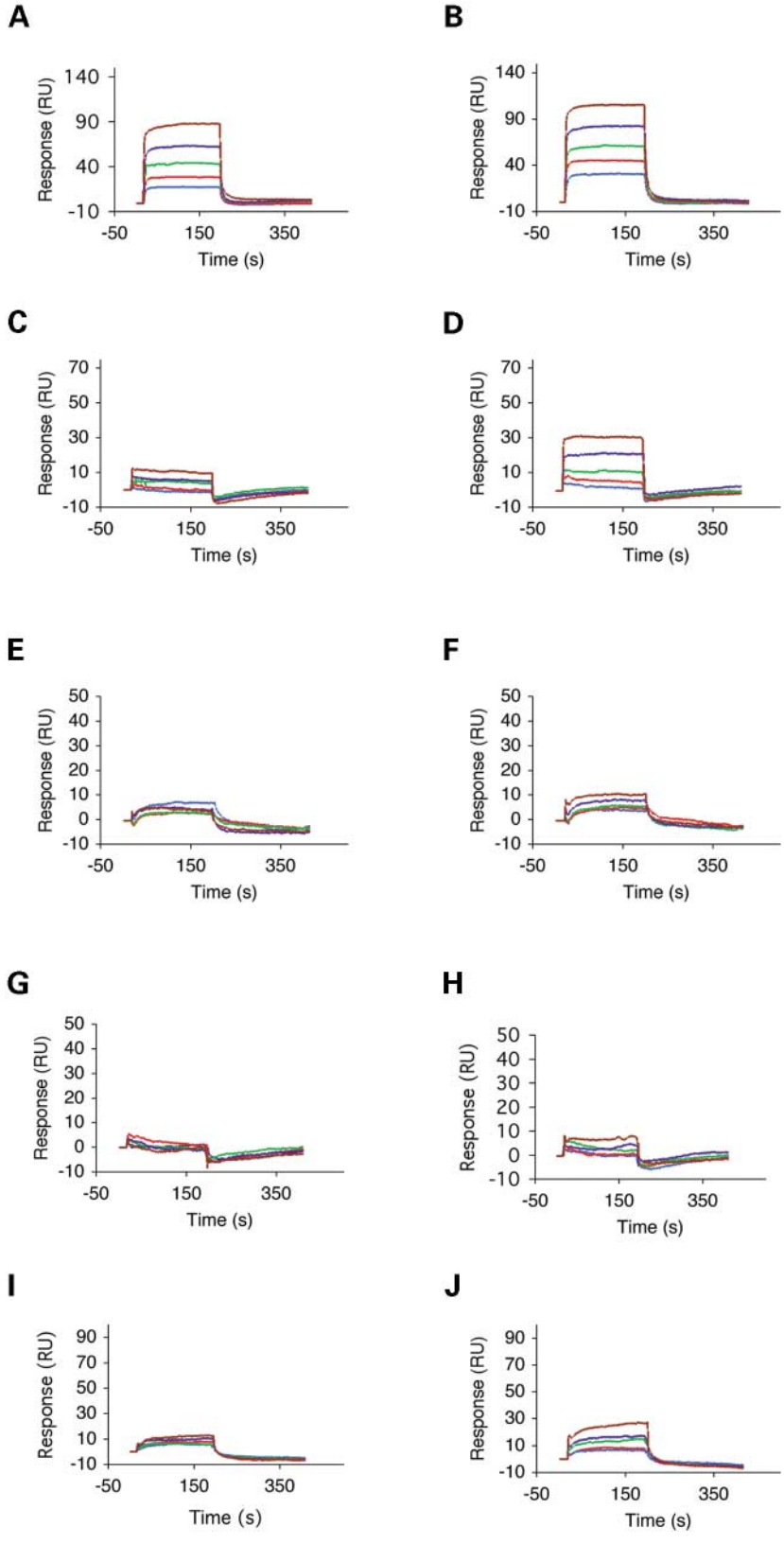

Figure 2. Surface plasmon resonance analysis of FGFR3c–FGF interactions. Sensorgrams of wild-type and Pro250Arg FGFR3c, respectively, binding to FGF1 (**A** and **B**), FGF2 (**C** and **D**), FGF4 (**E** and **F**), FGF7 (**G** and **H**) and FGF9 (**I** and **J**). Analyte concentrations are colored as follows: 25 nM in gray, 50 nM in blue, 100 nM in red, 200 nM in green, 400 nM in violet and 800 nM in brown. The biosensor chip response is indicated on the *y*-axis (ΔRU) as a function of time (*x*-axis) at 25°C.

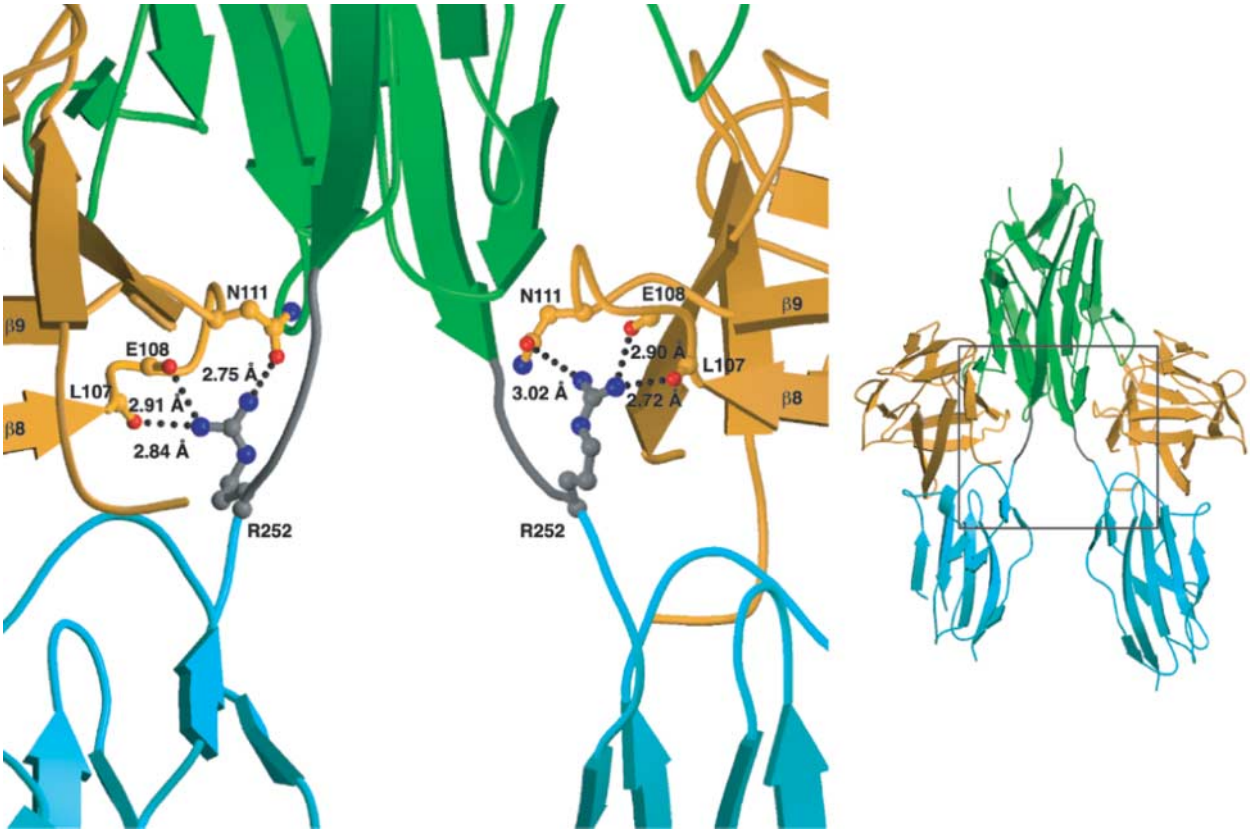

Figure 3. Gain-of-function hydrogen bonds in the Pro252Arg FGFR1c–FGF2 dimer. D2 and D3 of FGFR1c are shown in green and cyan, respectively. The D2–D3 linker is colored gray. FGF2 is shown in orange. Dotted lines represent hydrogen bonds. The hydrogen-bonding distances are indicated. On the right is a view of whole structure in the exact orientation as the detailed view shows, with the region of interest boxed.

of FGFR-related craniosynostosis syndromes or other pathological conditions.

MATERIALS AND METHODS

Protein expression and purification

Recombinant human FGFs, FGF1–FGF10 and FGF12b (FHF1b) were expressed in *Escherichia coli.* Soluble FGFs (FGF1, FGF2, FGF10 and FGF12) were purified by heparin affinity, ion exchange and size exclusion chromatography as described elsewhere (18,51–53). FGF7 was generously provided by Amgen (Amgen Inc.). Insoluble FGFs (FGF3, FGF5, FGF6 and FGF8) were refolded according to previously reported protocols and subsequently purified in a similar manner to soluble FGFs (54–56). FGF4 and FGF9 were purified through salt extraction and ammonium sulfate precipitation, respectively, and then purified as soluble FGFs (41,57).

The point mutations Pro252Arg and Pro250Arg were introduced into the minimal ligand-binding portion (D2–D3) of human FGFR1c (residues 142–365) and FGFR3c (residues 143–365), respectively, by using the Quik Change site-directed mutagenesis kit (Stratagene). Wild type and mutant receptors were expressed in *E. coli*, refolded *in vitro* and purified according to a previously reported protocol (51). Additional purification of wild type and mutant receptors was achieved through size-exclusion chromatography. Protein concentration was determined by mixing the protein solution with denaturing buffer (6.0 M guanidinium hydrochloride, 0.02 M sodium phosphate buffer, pH 6.5) using a Beckman DU640B spectrophotometer (Beckman Coulter) to measure absorbance at 280 nm along with the extinction coefficient, obtained from the ProtParam tool (www.expasy.ch), to calculate corrected protein concentrations.

Surface plasmon resonance analysis of FGF–FGFR interactions

Wild type and mutant FGFR–FGF interactions were characterized using a BIAcore 3000 instrument (Biacore AB, Uppsala, Sweden). To obtain kinetic data for wild-type and mutant FGFR–FGF interactions, FGF ligands were immobilized on research grade CM 5 chips according to standard amine coupling protocol (Biacore AB, Uppsala, Sweden). Briefly, carboxymethyl groups on the CM5 chip surface were first activated using an injection pulse of 50 µl (flow rate, 5 µl/min) of an equimolar mix of *N*-ethyl-*N*-(dimethyaminopropyl) carbodiimide and *N*-hydroxysuccinimide (final concentration 0.05 M, mixed immediately prior to injection). Following activation, FGF ligand was diluted to 25 µg/ml in HBS-EP

buffer [0.01 M HEPES, 0.15 M NaCl, 3 mM EDTA, 0.005% polysorbate 20 (v/v), pH 7.4] or 100 mM sodium acetate (pH 4.5) buffer and injected over the activated biosensor surface. Excess unreacted sites on the sensor surface were deactivated with a 40 µl injection of 1 M ethanolamine. FGF1 was immobilized to approximately 1000 response units (RU). FGF8 was found to aggregate on the sensor chip surface and therefore could not be immobilized. The remaining FGFs were successfully immobilized to comparable RU levels after accounting for relative molecular weight differences. FGF12 (FHF1b), an FGF homologous factor (FHF) that does not bind FGFRs, was immobilized on reference flow cells as a control. To obtain kinetic data, different concentrations of analytes (wild-type and mutant FGFR) in HBS-EP buffer [0.01 M HEPES, 0.15 M NaCl, 3 mM EDTA, 0.005% polysorbate 20 (v/v), pH 7.4] were injected over the FGF sensor chips at a flow rate of 50 µl/min. At the end of each sample injection (180 s), HBS-EP buffer was passed over the sensor surface to monitor the dissociation phase. Following 180 s of dissociation, the sensor surface was fully regenerated by injection of 50 µl of 2 M NaCl in 100 mM sodium acetate buffer (pH 4.5).

SPR data analysis

Reference responses from the control flow cell, containing immobilized FGF12 (FHF1b), were subtracted from FGF flow cells for each analyte injection using BiaEvaluation software (Biacore AB, Uppsala, Sweden). The resulting sensorgrams were used for kinetic parameter determination by globally fitting the entire association and dissociation phases to a 1:1 interaction using BiaEvaluation software (Biacore AB, Uppsala, Sweden). Disturbances, at the beginning and end, of each analyte injection were excluded. A minimum of four different analyte concentrations was used to determine the kinetic parameters for each interaction. Following curve fitting, each sensorgram was manually examined for data quality. χ^2 was less than 10% of R_{max} for each fit.

Crystalization and data collection

Crystals of Pro252Arg FGFR1c in complex with FGF2 were obtained using similar conditions to the previously reported crystallization conditions for wild type FGFR1c in complex with FGF2 (51). Two microliters of protein solution [10 mg/ml in 25 mM HEPES-NaOH (pH 7.5) and 150 mM NaCl] were mixed with 2 µl of the crystallization buffer consisting of 1.4 M ammonium sulfate, 22% glycerol in 0.1 M Tris–HCl (pH 8.5) at 23°C. Pro252Arg FGFR1c–FGF2 crystals belong to the tetragonal space group $P4_12_12$ and contain two FGFR1c–FGF2 complexes in the asymmetric unit. The unit cell dimensions are as follows: $a = b = 98.202$ Å, $c = 197.174$ Å, $\alpha = \beta = \gamma = 90°$. A 2.9 Å data set for the Pro252Arg mutant FGFR1c–FGF2 complex was collected from a flash frozen crystal (in a dry nitrogen stream) on a CCD detector at beamline X-4A at the National Synchrotron Light Source, Brookhaven National Laboratory. Data were processed using DENZO and SCALEPACK (58).

Structure determination and refinement of Pro252Arg FGFR1c-FGF2 complex

Molecular replacement solutions for the two copies of FGFR1c–FGF2 complex in the unit cells of Pro252Arg FGFR1c–FGF2 crystals were found with AmoRe (59) using the structure of wild-type FGFR1c complexed with FGF2 (51) (Protein Data Bank identification code 1CVS) as the search model. Tight non-crystallographic symmetry restraints were imposed throughout the refinement for the backbone atoms of FGF2, D2 and D3. Simulated annealing and positional/B factor refinement were performed using CNS (60). Model building into 2Fo – Fc and Fo – Fc electron density maps was performed with program O (61). The average B factor for all the protein atoms is 32.5 Å^2.

ACKNOWLEDGEMENTS

The authors acknowledge C. Basilico and S. Hubbard for comments and helpful discussions. Beamline X4A at the National Synchrotron Light Source, a DOE facility, is supported by the Howard Hughes Medical Institute. This work was sponsored in part by National Institute of Health grants DE13686 (M.M.) and HL52622 (R.J.L.).

REFERENCES

1. Jaye, M., Schlessinger, J. and Dionne, C.A. (1992) Fibroblast growth factor receptor tyrosine kinases: molecular analysis and signal transduction. *Biochim. Biophys. Acta.*, **1135**, 185–199.
2. Johnson, D.E., Williams, L.T., Gritli-Linde, A., Lewis, P., McMahon, A.P. and Linde, A. (1993) Structural and functional diversity in the FGF receptor multigene family. *Adv. Cancer Res.*, **60**, 1–41.
3. Ornitz, D.M., Xu, J., Colvin, J.S., McEwen, D.G., MacArthur, C.A., Coulier, F., Gao, G. and Goldfarb, M. (1996) Receptor specificity of the fibroblast growth factor family. *J. Biol. Chem.*, **271**, 15292–15297.
4. Yayon, A., Klagsbrun, M., Esko, J.D., Leder, P. and Ornitz, D.M. (1991) Cell surface, heparin-like molecules are required for binding of basic fibroblast growth factor to its high affinity receptor. *Cell*, **64**, 841–848.
5. Rapraeger, A.C., Krufka, A. and Olwin, B.B. (1991) Requirement of heparan sulfate for bFGF-mediated fibroblast growth and myoblast differentiation. *Science*, **252**, 1705–1708.
6. Ornitz, D.M., Yayon, A., Flanagan, J.G., Svahn, C.M., Levi, E. and Leder, P. (1992) Heparin is required for cell-free binding of basic fibroblast growth factor to a soluble receptor and for mitogenesis in whole cells. *Mol. Cell. Biol.*, **12**, 240–247.
7. Schlessinger, J., Plotnikov, A.N., Ibrahimi, O.A., Eliseenkova, A.V., Yeh, B.K., Yayon, A., Linhardt, R.J. and Mohammadi, M. (2000) Crystal structure of a ternary FGF-FGFR-heparin complex reveals a dual role for heparin in FGFR binding and dimerization. *Mol. Cell*, **6**, 743–750.
8. Muenke, M. and Wilkie, A.O. (2001) Craniosynostosis Syndromes. In Scriver, C.R., Beaudet, A.L., Valle, D., Sly, W.S., Childs, Kinzler, K. and Vogelstein, B. (eds.), *The Metabolic and Molecular Bases of Inherited Disease.* McGraw-Hill, New York, NY, Vol. IV, pp. 6117–6146.
9. Passos-Bueno, M.R., Wilcox, W.R., Jabs, E.W., Sertie, A.L., Alonso, L.G. and Kitoh, H. (1999) Clinical spectrum of fibroblast growth factor receptor mutations. *Hum. Mutat.*, **14**, 115–125.
10. Kan, S.H., Elanko, N., Johnson, D., Cornejo-Roldan, L., Cook, J., Reich, E.W., Tomkins, S., Verloes, A., Twigg, S.R., Rannan-Eliya, S. *et al.* (2002) Genomic screening of fibroblast growth-factor receptor 2 reveals a wide spectrum of mutations in patients with syndromic craniosynostosis. *Am. J. Hum. Genet.*, **70**, 472–486.
11. Neilson, K.M. and Friesel, R. (1996) Ligand-independent activation of fibroblast growth factor receptors by point mutations in the extracellular, transmembrane, and kinase domains. *J. Biol. Chem.*, **271**, 25049–25057.

12. Neilson, K.M. and Friesel, R.E. (1995) Constitutive activation of fibroblast growth factor receptor-2 by a point mutation associated with Crouzon syndrome. *J. Biol. Chem.*, **270**, 26037–26040.
13. Galvin, B.D., Hart, K.C., Meyer, A.N., Webster, M.K. and Donoghue, D.J. (1996) Constitutive receptor activation by Crouzon syndrome mutations in fibroblast growth factor receptor (FGFR)2 and FGFR2/Neu chimeras. *Proc. Natl Acad. Sci. USA*, **93**, 7894–7899.
14. Li, Y., Mangasarian, K., Mansukhani, A. and Basilico, C. (1997) Activation of FGF receptors by mutations in the transmembrane domain. *Oncogene*, **14**, 1397–1406.
15. Webster, M.K. and Donoghue, D.J. (1997) FGFR activation in skeletal disorders: too much of a good thing. *Trends Genet.*, **13**, 178–182.
16. Mohammadi, M., Schlessinger, J. and Hubbard, S.R. (1996) Structure of the FGF receptor tyrosine kinase domain reveals a novel autoinhibitory mechanism. *Cell*, **86**, 577–587.
17. Anderson, J., Burns, H.D., Enriquez-Harris, P., Wilkie, A.O. and Heath, J.K. (1998) Apert syndrome mutations in fibroblast growth factor receptor 2 exhibit increased affinity for FGF ligand. *Hum. Mol. Genet.*, **7**, 1475–1483.
18. Ibrahimi, O.A., Eliseenkova, A.V., Plotnikov, A.N., Yu, K., Ornitz, D.M. and Mohammadi, M. (2001) Structural basis for fibroblast growth factor receptor 2 activation in Apert syndrome. *Proc. Natl Acad. Sci. USA*, **98**, 7182–7187.
19. Yu, K., Herr, A.B., Waksman, G. and Ornitz, D.M. (2000) Loss of fibroblast growth factor receptor 2 ligand-binding specificity in Apert syndrome. *Proc. Natl Acad. Sci. USA*, **97**, 14536–14541.
20. Oldridge, M., Zackai, E.H., McDonald-McGinn, D.M., Iseki, S., Morriss-Kay, G.M., Twigg, S.R., Johnson, D., Wall, S.A., Jiang, W., Theda, C. *et al.* (1999) De novo alu-element insertions in FGFR2 identify a distinct pathological basis for Apert syndrome. *Am. J. Hum. Genet.*, **64**, 446–461.
21. Wilkie, A.O., Slaney, S.F., Oldridge, M., Poole, M.D., Ashworth, G.J., Hockley, A.D., Hayward, R.D., David, D.J., Pulleyn, L.J., Rutland, P. *et al.* (1995) Apert syndrome results from localized mutations of FGFR2 and is allelic with Crouzon syndrome. *Nat. Genet.*, **9**, 165–172.
22. Muenke, M., Schell, U., Hehr, A., Robin, N.H., Losken, H.W., Schinzel, A., Pulleyn, L.J., Rutland, P., Reardon, W., Malcolm, S. *et al.* (1994) A common mutation in the fibroblast growth factor receptor 1 gene in Pfeiffer syndrome. *Nat. Genet.*, **8**, 269–274.
23. Bellus, G.A., Gaudenz, K., Zackai, E.H., Clarke, L.A., Szabo, J., Francomano, C.A. and Muenke, M. (1996) Identical mutations in three different fibroblast growth factor receptor genes in autosomal dominant craniosynostosis syndromes. *Nat. Genet.*, **14**, 174–176.
24. Roscioli, T., Flanagan, S., Kumar, P., Masel, J., Gattas, M., Hyland, V.J. and Glass, I.A. (2000) Clinical findings in a patient with FGFR1 P252R mutation and comparison with the literature. *Am. J. Med. Genet.*, **93**, 22–28.
25. Lomri, A., Lemonnier, J., Hott, M., de Parseval, N., Lajeunie, E., Munnich, A., Renier, D. and Marie, P.J. (1998) Increased calvaria cell differentiation and bone matrix formation induced by fibroblast growth factor receptor 2 mutations in Apert syndrome. *J. Clin. Invest.*, **101**, 1310–1317.
26. Dell, K.R. and Williams, L.T. (1992) A novel form of fibroblast growth factor receptor 2. Alternative splicing of the third immunoglobulin-like domain confers ligand binding specificity. *J. Biol. Chem.*, **267**, 21225–21229.
27. Miki, T., Bottaro, D.P., Fleming, T.P., Smith, C.L., Burgess, W.H., Chan, A.M. and Aaronson, S.A. (1992) Determination of ligand-binding specificity by alternative splicing: two distinct growth factor receptors encoded by a single gene. *Proc. Natl Acad. Sci. USA*, **89**, 246–250.
28. Yayon, A., Zimmer, Y., Shen, G.H., Avivi, A., Yarden, Y. and Givol, D. (1992) A confined variable region confers ligand specificity on fibroblast growth factor receptors: implications for the origin of the immunoglobulin fold. *EMBO J.*, **11**, 1885–1890.
29. Zhou, Y.X., Xu, X., Chen, L., Li, C., Brodie, S.G. and Deng, C.X. (2000) A Pro250Arg substitution in mouse Fgfr1 causes increased expression of Cbfa1 and premature fusion of calvarial sutures. *Hum. Mol. Genet.*, **9**, 2001–2008.
30. Chellaiah, A., Yuan, W., Chellaiah, M. and Ornitz, D.M. (1999) Mapping ligand binding domains in chimeric fibroblast growth factor receptor molecules. Multiple regions determine ligand binding specificity. *J. Biol. Chem.*, **274**, 34785–34794.
31. Pantoliano, M.W., Horlick, R.A., Springer, B.A., Van Dyk, D.E., Tobery, T., Wetmore, D.R., Lear, J.D., Nahapetian, A.T., Bradley, J.D. and Sisk, W.P. (1994) Multivalent ligand-receptor binding interactions in the fibroblast growth factor system produce a cooperative growth factor and heparin mechanism for receptor dimerization. *Biochemistry*, **33**, 10229–10248.
32. Hoshikawa, M., Yonamine, A., Konishi, M. and Itoh, N. (2002) FGF-18 is a neuron-derived glial cell growth factor expressed in the rat brain during early postnatal development. *Brain Res. Mol. Brain Res.*, **105**, 60–66.
33. Ohmachi, S., Mikami, T., Konishi, M., Miyake, A. and Itoh, N. (2003) Preferential neurotrophic activity of fibroblast growth factor-20 for dopaminergic neurons through fibroblast growth factor receptor-1c. *J. Neurosci. Res.*, **72**, 436–443.
34. Santos-Ocampo, S., Colvin, J.S., Chellaiah, A. and Ornitz, D.M. (1996) Expression and biological activity of mouse fibroblast growth factor-9. *J. Biol. Chem.*, **271**, 1726–1731.
35. Ornitz, D.M. and Leder, P. (1992) Ligand specificity and heparin dependence of fibroblast growth factor receptors 1 and 3. *J. Biol. Chem.*, **267**, 16305–16311.
36. Chellaiah, A.T., McEwen, D.G., Werner, S., Xu, J. and Ornitz, D.M. (1994) Fibroblast growth factor receptor (FGFR) 3. Alternative splicing in immunoglobulin-like domain III creates a receptor highly specific for acidic FGF/FGF-1. *J. Biol. Chem.*, **269**, 11620–11627.
37. Lin, H.Y., Kaplow, J., Jaye, M. and Hayman, M.J. (1997) Ligand-binding specificity of human fibroblast growth factor receptor-3 IIIc. *FEBS Lett.*, **411**, 389–392.
38. Shimizu, A., Tada, K., Shukunami, C., Hiraki, Y., Kurokawa, T., Magane, N. and Kurokawa-Seo, M. (2001) A novel alternatively spliced fibroblast growth factor receptor 3 isoform lacking the acid box domain is expressed during chondrogenic differentiation of ATDC5 cells. *J. Biol. Chem.*, **276**, 11031–11040.
39. Kim, H.J., Rice, D.P., Kettunen, P.J. and Thesleff, I. (1998) FGF-, BMP- and Shh-mediated signalling pathways in the regulation of cranial suture morphogenesis and calvarial bone development. *Development*, **125**, 1241–1251.
40. Rice, D.P., Aberg, T., Chan, Y., Tang, Z., Kettunen, P.J., Pakarinen, L., Maxson, R.E. and Thesleff, I. (2000) Integration of FGF and TWIST in calvarial bone and suture development. *Development*, **127**, 1845–1855.
41. Plotnikov, A.N., Eliseenkova, A.V., Ibrahimi, O.A., Shriver, Z., Sasisekharan, R., Lemmon, M.A. and Mohammadi, M. (2001) Crystal structure of fibroblast growth factor 9 reveals regions implicated in dimerization and autoinhibition. *J. Biol. Chem.*, **276**, 4322–4329.
42. Colvin, J.S., Green, R.P., Schmahl, J., Capel, B. and Ornitz, D.M. (2001) Male-to-female sex reversal in mice lacking fibroblast growth factor 9. *Cell*, **104**, 875–889.
43. Warren, S.M., Greenwald, J.A., Spector, J.A., Bouletreau, P., Mehrara, B.J. and Longaker, M.T. (2001) New developments in cranial suture research. *Plast. Reconstr. Surg.*, **107**, 523–540.
44. Glaser, R.L., Broman, K.W., Schulman, R.L., Eskenazi, B., Wyrobek, A.J. and Jab, E.W. (2003) The paternal-age effect in Apert syndrome is due, in part, to the increased frequency of mutations in sperm. *Am. J. Hum. Genet.*, **73**, 939–947.
45. Goriely, A., McVean, G.A.T., Rojmyr, M., Ingemarsson, B. and Wilkie, A.O.M. (2003) Evidence for selective advantage of pathogenic FGFR2 mutations in the male germ line. *Science*, **301**, 643–646.
46. Tiemann-Boege, I., Navidi, W., Grewal, R., Cohn, D., Eskenazi, B., Wyrobek, A.J. and Arnheim, N. (2002) The observed human sperm mutation frequency cannot explain the achondroplasia paternal age effect. *Proc. Natl Acad. Sci. USA*, **99**, 14952–14957.
47. Slaney, S.F., Oldridge, M., Hurst, J.A., Moriss-Kay, G.M., Hall, C.M., Poole, M.D. and Wilkie, A.O. (1996) Differential effects of FGFR2 mutations on syndactyly and cleft palate in Apert syndrome. *Am. J. Hum. Genet.*, **58**, 923–932.
48. Lajeunie, E., Cameron, R., El Ghouzzi, V., de Parseval, N., Journeau, P., Gonzales, M., Delezoide, A.L., Bonaventure, J., Le Merrer, M. and Renier, D. (1999) Clinical variability in patients with Apert's syndrome. *J. Neurosurg.*, **90**, 443–447.
49. von Gernet, S., Golla, A., Ehrenfels, Y., Schuffenhauer, S. and Fairley, J.D. (2000) Genotype-phenotype analysis in Apert syndrome suggests opposite effects of the two recurrent mutations on syndactyly and outcome of craniofacial surgery. *Clin. Genet.*, **57**, 137–139.

50. Yeh, B.K., Igarashi, M., Eliseenkova, A.V., Plotnikov, A.N., Sher, I., Ron, D., Aaronson, S.A. and Mohammadi, M. (2003) Structural basis by which alternative splicing confers specificity in fibroblast growth factor receptors. *Proc. Natl Acad. Sci. USA*, **100**, 2266–2271.
51. Plotnikov, A.N., Schlessinger, J., Hubbard, S.R. and Mohammadi, M. (1999) Structural basis for FGF receptor dimerization and activation. *Cell*, **98**, 641–650.
52. Igarashi, M., Finch, P.W. and Aaronson, S.A. (1998) Characterization of recombinant human fibroblast growth factor (FGF)-10 reveals functional similarities with keratinocyte growth factor (FGF-7). *J. Biol. Chem.*, **273**, 13230–13235.
53. Olsen, S.K., Garbi, M., Zampieri, N., Eliseenkova, A.V., Ornitz, D.M., Goldfarb, M. and Mohammadi, M. (2003) FHFs share structural but not functional homology to FGFs. *J. Biol. Chem.*, **278**, 34226–34236.
54. MacArthur, C.A., Lawshe, A., Xu, J., Santos-Ocampo, S., Heikinheimo, M., Chellaiah, A.T. and Ornitz, D.M. (1995) FGF-8 isoforms activate receptor splice forms that are expressed in mesenchymal regions of mouse development. *Development*, **121**, 3603–3613.
55. Pizette, S., Batoz, M., Prats, H., Birnbaum, D. and Coulier, F. (1991) Production and functional characterization of human recombinant FGF-6 protein. *Cell. Growth Differ.*, **2**, 561–566.
56. Clements, D.A., Wang, J.K., Dionne, C.A. and Goldfarb, M. (1993) Activation of fibroblast growth factor (FGF) receptors by recombinant human FGF-5. *Oncogene*, **8**, 1311–1316.
57. Bellosta, P., Iwahori, A., Plotnikov, A.N., Eliseenkova, A.V., Basilico, C. and Mohammadi, M. (2001) Identification of receptor and heparin binding sites in fibroblast growth factor 4 by structure-based mutagenesis. *Mol. Cell. Biol.*, **21**, 5946–5957.
58. Otwinowski, Z. and Minor, W. (1997) Processing of x-ray diffraction data collected in oscillation mode. *Methods Enzymol.*, **276**, 307–326.
59. Navaza, J. (1994) AMoRe: an automated package for molecular replacement. *Acta Crystallogr. A*, **50**, 157–163.
60. Brunger, A.T., Adams, P.D., Clore, G.M., DeLano, W.L., Gros, P., Grosse-Kunstleve, R.W., Jiang, J.S., Kuszewski, J., Nilges, M., Pannu, N.S. *et al.* (1998) Crystallography and NMR system: A new software suite for macromolecular structure determination. *Acta Crystallogr. D. Biol. Crystallogr.*, **54**, 905–921.
61. Jones, T.A., Zou, J.Y., Cowan, S.W. and Kjeldgaard, G. (1991) Improved methods for binding protein models in electron density maps and the location of errors in these models. *Acta Crystallogr. A.*, **47**, 110–119.